

Surface Displacement Detection Using Coherent Laser and Machine Vision

Mario Gonzalez*, Jim Williams, Claude Ratliff

Research and Development Department, Intouch Automation LLC, Novi, United States

Email address:

Mar_albert_21@hotmail.com (M. Gonzalez), Jwilliams@intouchautomation.com (J. Williams),

CRatliff@intouchautomation.com (C. Ratliff)

*Corresponding author

To cite this article:

Mario Gonzalez, Jim Williams, Claude Ratliff. Surface Displacement Detection Using Coherent Laser and Machine Vision. *Applied Engineering*. Vol. 5, No. 2, 2021, pp. 66-71. doi: 10.11648/j.ae.20210502.15

Received: October 6, 2021; **Accepted:** October 29, 2021; **Published:** November 5, 2021

Abstract: Ever since the discovery of the photoelectric theory and other inventions and discoveries, more and more devices that were only thought and designed to be in a laboratory environment since their inception have been migrating into the industrial environment because that environment has evolved and is absorbing laboratory grade equipment for easier inspection and faster, more accurate examinations. As a result, we have shorter analysis times and more exact, accurate, and repeatable measurements utilizing newer and fewer devices. These technologies allow for more advanced devices by merging different and sophisticated programming languages allowing these devices to become more and more versatile and making them easier to integrate with different industries and environments. In this document we intend to describe and explain mathematically and diagrammatically a new digital image processing algorithm considering different physical variables that can be easily adjusted or replaced with new individual components and different processing systems using only light projection, image capturing, and computational processing with all of them working together homogeneously to output different and tangible numbers for further and easier analysis. One these different examples is described, tested, analyzed, and explained in detail in this document using only the previously mentioned devices in an industrial environment.

Keywords: Laser, Surface Displacement, Artificial Vision, Machine Vision

1. Introduction

Since the discovery of the laser (Light Amplification by Stimulated Emission of Radiation) in 1917 with Albert Einstein's published paper "Zur Quantentheorie der Strahlung" (On the Quantum Theory of Radiation) using other approximation on Max Planck's law of radiation for the stimulated emission of electromagnetic radiation [1] the laser has been used in multiple industry based and laboratory fascinating applications; but, it was not until 1928 that Rudolf W. Ladenburg confirmed the existence of the phenomena of stimulated emission and negative absorption. They have been used in countless applications and for different purposes.

When using lasers in industrial applications, most of the time intrinsic laser properties are left aside; however, they must be considered to have a physical and appropriate approach to the real world. Some of these properties include, but are not limited to, coherence and collimation [2-3]. Nowadays, laser systems used in

the industry in conjunction with other devices such as cameras or detectors, computer vision turned into an interdisciplinary field that deals with how computers can gain high-level understanding from images and videos. In the industry from an engineering perspective, it tries to understand and automate tasks that the human vision can do [4-6] The computer vision starts with the acquisition, then processing and analyzing for the understanding of digital images for further high-dimensional data from the real world in order to produce numeral symbolic information for the decision making [7-10]. The image understanding can be seen as the disentangling of symbolic information from image data using physics and statistics [11].

Even with all these devices online, the decision making resides in a centralized brain, in industrial environments the most common and reliable device is a programmable logic controller (PLC). It is used for manufacturing processes, assembly lines, machines, robotic devices, or any other activity that requires high reliability, ease of programming and process fault diagnostic [12]. New tools have emerged in

the industry to make new devices or sensors. These devices and sensors have been evolving overtime migrating into new languages like Python. This language is an interpreted high-level general-purpose programming software. Its design emphasizes code readability using indentation and its language constructs as well as an object-oriented approach that aims to help programmers write clear, logical code for small- and large-scale projects. Today python ranks as one of the most popular programming languages. [13-15]

2. Mathematical Background

For the optical array to comply with the correct functionality of the laser, the coherence length cannot decay in the length of the array. The longer the coherence length is, the closer to a perfect sinusoidal wave it is going to be. To calculate this, the following formula must be evaluated.

$$L = \frac{2 \ln 2}{\pi} \frac{\lambda^2}{n \Delta \lambda}$$

Equation 1

Where n is the refractive index of the medium

$$n = \frac{c}{v}$$

Equation 2

And $\Delta \lambda$ is the full width at half the maximum value for the light source which can be calculated with the following equation

$$f(x) = \frac{1}{\sigma \sqrt{2\pi}} e^{-\frac{(x-x_0)^2}{2\sigma^2}}$$

Equation 3

Once the coherent length is obtained, we must make sure the degree of coherence is always maintained. The laser degree of coherence is calculated in its first order degree using the following equation.

$$g^{(1)}(r_1, t_1; r_2, t_2) = \frac{\langle E^*(r_1, t_1) E(r_2, t_2) \rangle}{[|E(r_1, t_1)|^2 |E(r_2, t_2)|^2]^{\frac{1}{2}}}$$

Equation 4

Where $\langle \dots \rangle$ is the statistical averages. If the evaluation plane gets restricted to $r = z$ for stationary states, it will not depend on t_1 , but on the time delay $\tau = t_1 - t_2 - \frac{z_1 - z_2}{c}$ only if $z_1 \neq z_2$. This condition allows us to write it as a simplified form.

$$g^{(1)}(\tau) = \frac{\langle E^*(t) E(t + \tau) \rangle}{\langle |E(t)|^2 \rangle}$$

Equation 5

After evaluating for a single frequency light like this case, a single frequency laser [16], we obtain

$$g^{(1)}(\tau) = e^{-j\omega_0 \tau}$$

Equation 6

For this specific application we are using a 562nm green laser which has a frequency of 71.7MHz and a coherence length of 1.33 meters. This means the laser in question is coherent in its

full length on the experimental array. An instance of the physical experimental array is shown in Figure 1.

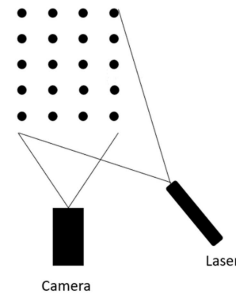


Figure 1. Experimental array.

Since the laser is projecting in an angle, geometrical transformations need to be done prior to the image processing. This can be achieved with rotational matrices like described in the following equation.

$$M = \begin{bmatrix} \cos\theta & -\sin\theta \\ \sin\theta & \cos\theta \end{bmatrix}$$

Equation 7

That rotation matrix describes the movement aligned to its center, in order to rotate off center, we will use the following equation [17].

$$\begin{pmatrix} \alpha & \beta & (1 - \alpha) \cdot center_x - \beta \cdot center_y \\ -\beta & \alpha & \beta \cdot center_x + (1 - \alpha) \cdot center_y \end{pmatrix}$$

Equation 8

Where

$$\alpha = scale \cdot \cos\theta$$

$$\beta = scale \cdot \sin\theta$$

Equation 9

After the geometrical transformations we can modify any abnormalities on the grid as shown in Figure 2.[18-19]

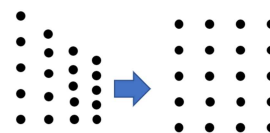


Figure 2. Grid pattern before and after geometrical transformations.

The specific coordinates of each dot can be calculated with simple trigonometry identities as seen in Figure 3.

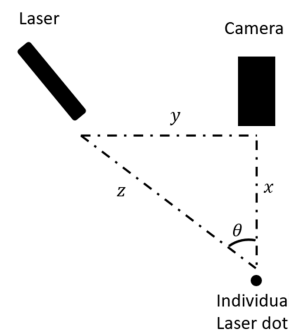


Figure 3. Extrapolation of a single dot array.

Where

$$\theta_n = \arctan\left(\frac{x_n}{y_n}\right)$$

Equation 10

The subscript n denotes each individual dot, the distance y is a constant in the optical array; whereas x can change over time if the surface in which the laser hits move.

While processing the images, a mask is applied for the specific band of frequency for the laser, making analysis easier.

$$A(x, y) \Rightarrow A^\alpha(x, y)$$

Equation 11

Once the new matrix is composed of components working at the laser frequency, a sample is taken to reference the next frames. This sample is shown in Figure 4.

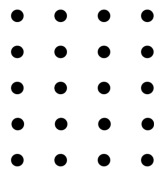


Figure 4. Initial dot array working as a sample.

This sample $A(x, y)$ is going to help keep track of the displacement based on the movement of the surface. Once the sample $A^\alpha(x, y)$ is taken, any displacement that occurred on the surface will distort the dot pattern like shown in Figure 5.

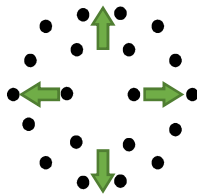


Figure 5. Displaced pattern by surface movement.

Once the displaced surface image $A^\alpha_\Delta(x, y)$ is taken, it can be compared to the original. This is shown in Figure 6.

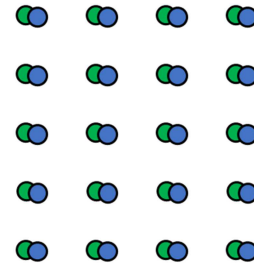


Figure 6. Original dots are shown in green, New displaced surface dots are shown in blue.

Once $A^\alpha(x, y)$ and $A^\alpha_\Delta(x, y)$ we can find out how much it has moved over Δ_t by performing

$$A^\alpha_\Delta(x, y)_{t1} - A^\alpha(x, y)_{t2}$$

Equation 12

This mathematical operation is shown in Figure 7.



Figure 7. The subtraction is shown in the picture and the resulting figure can correlate over time and space.

In the end, an algorithm can be produced based on these steps previously described and the final calculation can be pushed into another processing device for automation purposes. This algorithm can be seen in Figure 8.

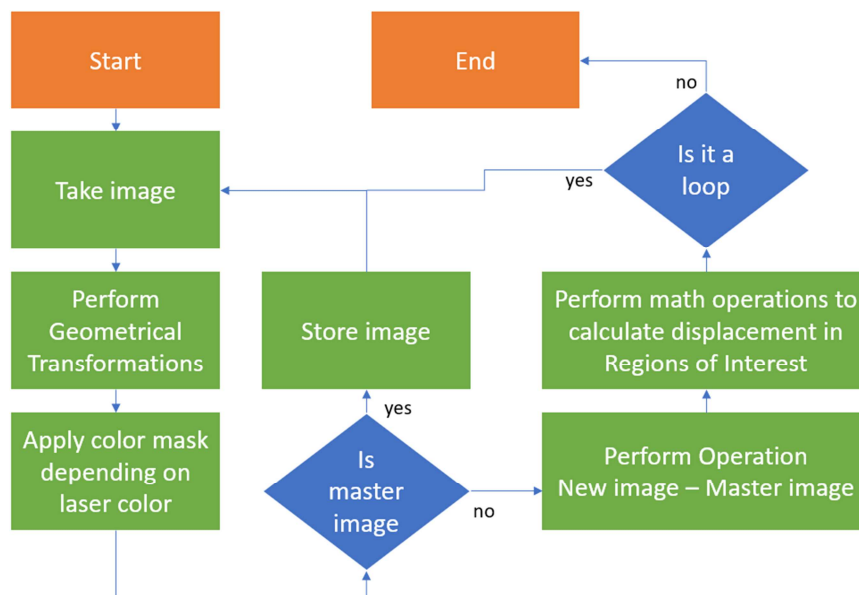


Figure 8. Algorithm for displacement calculation based on digital image processing.

3. Application

A simple application is to analyze a leather surface for functionality. Figure 9 shows a surface with a lot of irregularities like stitching, perforated patches, and seams. The surface must move in patterns and displace only to a certain point.



Figure 9. Test surface.

The first step is to shine a laser or several lasers at the target surface remembering all the lasers must be always coherent at the target distance to avoid optical irregularities. This is shown in Figure 10.



Figure 10. Coherent laser hitting the target surface.

Once the surface it hit with the lasers and we have verified the laser is coherent, the optical array from Figure 3 must be replicated, the camera resolution for this application was chosen to be 1920x1080 pixels and the graphics processor running Linux with ARM 64-bit processor architecture. The algorithm from Figure 8 must be modified in order to process these movements and validate all results at once. This modified algorithm is shown in Figure 11.

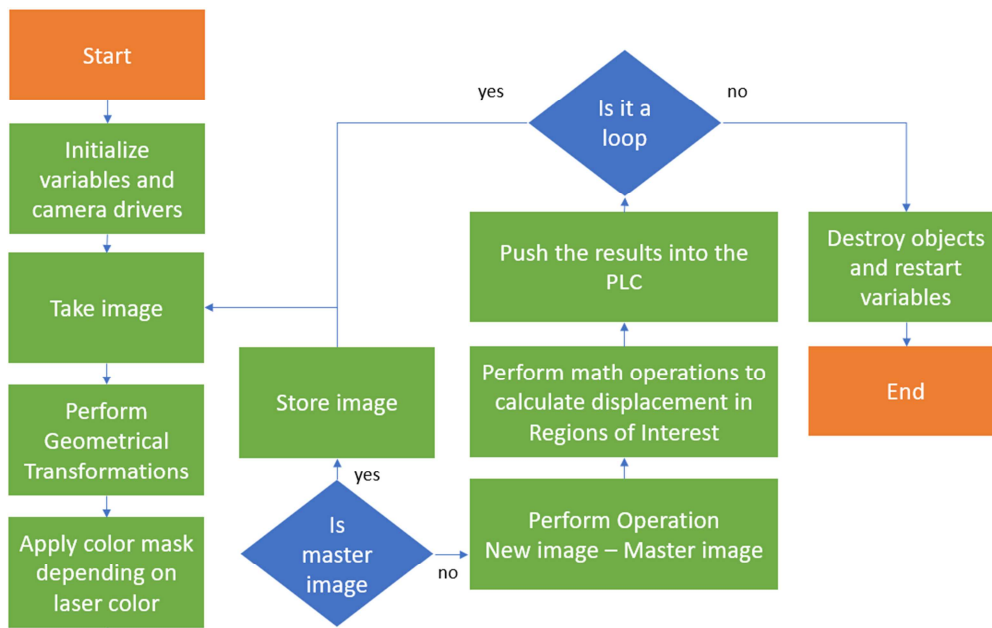


Figure 11. Modified algorithm to this specific application.

Once the processing is done, we can visualize the surface displacement like shown in Figure 12.

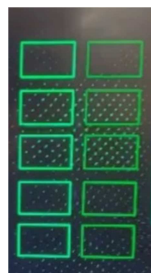


Figure 12. Processed image showing displacement on the surface.

In this case the value pushed into the PLC is the mean value of the illuminated pixels for each one of the regions of interest following Equation 13.

$$A = \frac{1}{n} \sum_{i=1}^n x_i$$

Equation 13

Where n is the number of terms and x_i is the value of each individual item in the list of numbers being averaged. The PLC then makes the decision of whether the part is good or bad.

For the processing times in this example, the code was

optimized for the ARM 64-bit processor and running the routine we performed a benchmark doing 287 iterations and getting an average of 10.13307571ms per frame. This is shown in Figure 13.

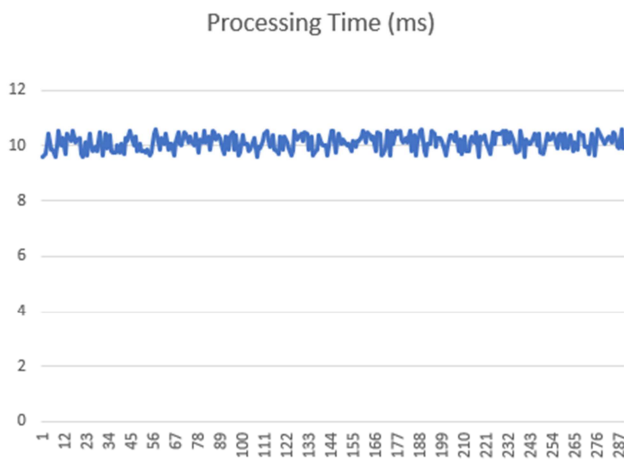


Figure 13. Processing time on the 287 frames.

Having evaluated the performance of this ARM 64-bit processor, we moved on to an ARM 64-bit with 384-core CUDA CORES GPU with 48 Tensor Cores giving us a total of 2.632172777ms per frame. The chart is shown in Figure 14.

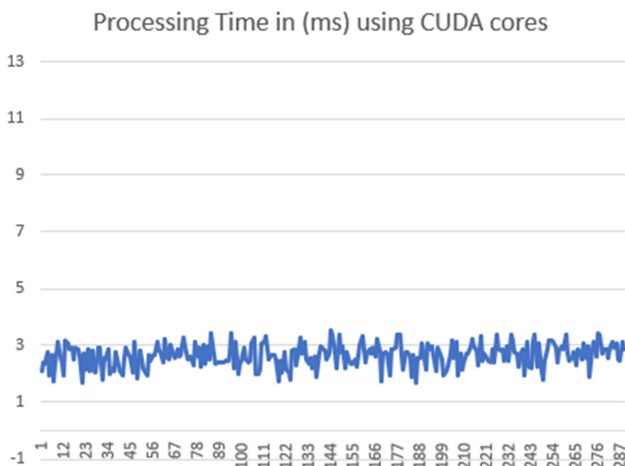


Figure 14. Processing time on the 287 frames using cuda cores.

Having this number and using a sequence of timers, we can obtain the displacement per second either advancing or retracting. This is just one of the countless applications for this proposed method. The head of the laser can be changed to a diffractive pattern using straight lines or an even bigger array of dots putting more resolution into the system.

4. Conclusion

The results obtained from the experimental setup are consistent and repeatable. Using a simple camera, a diffracted laser beam and a small computer, we can obtain a high-speed input for different field applications like displacement over time, presence of objects, and several

other different coefficients derived from time and space interactions. Ambient light can affect the measurement if it ever reaches the laser wavelength and power. The lens aperture can help reduce the affects of ambient light, but the surface must be shielded from the ambient light to avoid any discrepancies because of light exposure and occlusion. Minor vibrations do not affect the measurement if the amount of surface displacement is much greater than the movement caused by the vibrations. The surface can be lifted or isolated from any other moving surfaces to avoid any other vibrations during testing. A few of the advantages of using a computer for processing is the versatility and scalability for recording, capture, and storage of tests for later verification. Different types of cameras and lasers can be used depending on the setup for better results. As technology progresses, the processing times will keep diminishing until it can be performed in real time using more and more inputs for the system to process at the same time.

References

- [1] A. Einstein, "Zur Quantentheorie der Strahlung," *Phys. Z.*, vol. 18, pp. 121-128, 1917.
- [2] W. Emil., "Introduction to the theory of coherence and polarization of light.," *Cambridge University Press ISBN 9780521822114.*, 2007.
- [3] M. Griot, "Introduction to Laser Technology," *Melles Griot Catalog*, p. 36, 2018.
- [4] D. H. Ballard and C. M. Brown, "Computer Vision," *ISBN 978-0-13-165316-0.*, 1982.
- [5] T. Huang, "Computer Vision: Evolution And Promise," *Geneva: CERN*, Vols. doi: 10.5170/CERN-1996-008.21. ISBN 978-9290830955., p. 21–25, 1996.
- [6] M. Sonka, V. Hlavac and R. Boyle, "Image Processing, Analysis, and Machine Vision," *ISBN 978-0-495-08252-1.*, 2008.
- [7] R. Klette, "Concise Computer Vision," *ISBN 978-1-4471-6320-6.*, 2014.
- [8] L. G. Shapiro and G. C. Stockman, "Computer Vision," *ISBN 978-0-13-030796-5.*, 2001.
- [9] T. Morris, "Computer Vision and Image Processing.," *ISBN 978-0-333-99451-1.*, 2004.
- [10] B. Jähne and H. Haußecker, "Computer Vision and Applications, A Guide for Students and Practitioners.," *ISBN 978-0-13-085198-7.*, 2000.
- [11] D. A. Forsyth and J. Ponce, "Computer Vision, A Modern Approach," *ISBN 978-0-13-085198-7*, 2003.
- [12] S. P. Tubbs, "Programmable Logic Controller (PLC) Tutorial, Siemens Simatic S7-1200.," *Publicis MCD Werbeagentur GmbH; 3rd ed*, 2018.
- [13] pypl.github.io, *PYPL Popularity of Programming Language index*, 2017.
- [14] S. Overflow, *Stack Overflow Developer Survey 2020*, Stack Overflow, 2021.

- [15] J. D. T. f. P. a. Teams., *The State of Developer Ecosystem in 2020 Infographic*, 2021.
- [16] R. Loudon, *The Quantum Theory of Light*, Oxford: Oxford University Press, 2000.
- [17] P. Lounesto, *Clifford algebras and spinors*, Cambridge: Cambridge University Press, 2001.
- [18] R. O. Duda and P. E. Hart, "Use of the Hough transformation to detect lines and curves in pictures," *Communications of the ACM*, vol. 15, no. 1, 1972.
- [19] D. Kuhlman, "A Python Book: Beginning Python, Advanced Python, and Python Exercises," 2012.